Research Square

Preprints are preliminary reports that have not undergone peer review.
They should not be considered conclusive, used to inform clinical practice,
or referenced by the media as validated information.

The Rotor-Bivector Orbit Atlas: A Geometric Algebra Framework for Classifying Orbits in Axisymmetric and Triaxial Galactic Potentials

Hicham Banouh

h.banouh@univ-bouira.dz

University of Bouira

Research Article

Keywords: Geometric Algebra, Clifford Algebra, Galactic Dynamics, Hamiltonian Systems, Bivectors, Rotors

Posted Date: September 11th, 2026

DOI: https://doi.org/10.21203/rs.3.rs-10882889/v1

License: This work is licensed under a Creative Commons Attribution 4.0 International License.
Read Full License

Additional Declarations: No competing interests reported.

The Rotor–Bivector Orbit Atlas: A Geometric Algebra Framework for Classifying Orbits in Axisymmetric and Triaxial Galactic Potentials

Hicham Banouh[1*]

[1*]Department of Mathematics, Faculty of Exact Sciences, University of Bouira, Bouira, 10000, Algeria.

Corresponding author(s). E-mail(s): h.banouh@univ-bouira.dz;

Abstract

We construct a rigorous geometric algebra framework for classifying orbits in analytic Hamiltonian systems on $\mathbb{R}^{\mathbf{3}}$, with applications to axisymmetric and triaxial galactic potentials. By representing the angular momentum as a bivector $\mathbf{L} = \mathbf{x} \wedge \mathbf{p} \in \bigwedge^{\mathbf{2}} \mathbb{R}^{\mathbf{3}}$, the space of oriented orbital planes is identified with the real projective plane $\mathbb{R}\boldsymbol{P}^{\mathbf{2}}$. We resolve the kinematic singularities inherent in Euler-angle parametrizations by evolving the system on the spin group $\mathbf{Spin(3)}$. For integrable Stackel potentials, we establish a Bivector Spectral Theorem demonstrating that the time evolution of $\mathbf{L}(\boldsymbol{t})$ decomposes into an orthogonal sum of independently rotating bivector components, yielding an $\boldsymbol{O(N)}$ algebraic frequency extraction algorithm. We define the Rotor-Bivector Atlas as a continuous mapping from the orbit space to $\mathbb{R}\boldsymbol{P}^{\mathbf{2}} \times \mathbb{R}_{\geq \mathbf{0}}$, prove its topological stability under $\boldsymbol{C}^{\boldsymbol{k}}$ perturbations away from integrability, and provide a rigorous Diophantine approximation criterion for algebraic resonance detection.

Keywords: Geometric Algebra, Clifford Algebra, Galactic Dynamics, Hamiltonian Systems, Bivectors, Rotors

MSC Classification: 70F15 , 15A66 , 37N05 , 85A05

1 Introduction

The classification of bounded trajectories in Hamiltonian systems on $\mathbb{R}^6$ fundamentally relies on the geometry of the angular momentum vector. In standard astrophysical

formulations, angular momentum is treated as a pseudovector in $\mathbb{R}^3$, and its evolution is tracked via rotation matrices in $SO(3)$ or Euler angles. This approach introduces two mathematical obstructions: the kinematic singularity of Euler angles (gimbal lock), and the algebraic opacity of separating rotational modes in non-integrable potentials.

Geometric algebra (GA) provides a singularity-free representation of rotations via the spin group Spin(3), identified with the unit rotors in the even subalgebra of the Clifford algebra $\mathcal{C}\ell_{3,0}$. In this language, the angular momentum is naturally a bivector $\mathbf{L} = \mathbf{x} \wedge \mathbf{p} \in \bigwedge^2 \mathbb{R}^3$, and its evolution is governed by a linear differential equation on the Lie algebra $\mathfrak{so}(3) \cong \bigwedge^2 \mathbb{R}^3$.

In this paper, we formalize this observation into a rigorous mathematical framework, resolving several foundational issues in prior heuristic approaches to GA in astrophysics. Our principal results are:

- **Theorem 2**: A precise resolution of the angular velocity bivector $\mathbf{\Omega}$ from the torque $\boldsymbol{\tau} = \dot{\mathbf{L}}$ via orthogonal projection in $\mathfrak{so}(3)$, correcting prior algebraic errors in the literature regarding bivector inversion.
- **Theorem 3** (Bivector Spectral Theorem): For Stackel potentials, proving that $\mathbf{L}(t)$ admits an orthogonal decomposition into three bivector components rotating at the fundamental frequencies, allowing exact frequency extraction without Fourier transforms.
- **Theorem 5**: The construction of the Rotor-Bivector Atlas as a continuous map on $\mathbb{R}P^2$, with a rigorous continuity bound demonstrating topological stability under KAM perturbations.
- **Theorem 7**: A formal proof that bivector frequency extraction has linear complexity. Its $O(N)$ cost improves on the $O(N \log N)$ cost of spectral methods.

The paper is structured as follows. Section 2 establishes the notation and algebraic preliminaries of $\mathcal{C}\ell_{3,0}$. Section 3 derives the exact rotor dynamics and resolves the angular velocity extraction. Section 4 tackles the integrable Stackel case, establishing the spectral theorem. Section 5 defines the atlas on $\mathbb{R}P^2$ and proves its stability. Section 6 details algebraic resonance detection, and Section 7 proves the computational bounds, verified numerically in Section 8.

2 Geometric Preliminaries and Notation

To ensure complete mathematical precision, we consolidate all notation and algebraic definitions here. A summary is provided in Table 1.

Definition 1 (Clifford Algebra $\mathcal{C}\ell_{3,0}$) Let $\{\mathbf{e}_1, \mathbf{e}_2, \mathbf{e}_3\}$ be an orthonormal basis for $\mathbb{R}^3$ with the positive-definite quadratic form, satisfying the geometric product relation $\mathbf{e}_i\mathbf{e}_j + \mathbf{e}_j\mathbf{e}_i = 2\delta_{ij}$. The algebra $\mathcal{C}\ell_{3,0}$ is graded as:

$$\mathcal{C}\ell_{3,0} = \mathbb{R} \oplus \mathbb{R}^3 \oplus \bigwedge^2 \mathbb{R}^3 \oplus \bigwedge^3 \mathbb{R}^3 \tag{1}$$

consisting of scalars (grade 0), vectors (grade 1), bivectors (grade 2), and pseudoscalars (grade 3).

Table 1 Primary Symbol Register

Symbol	Definition / Meaning
$\mathcal{C}\ell_{3,0}$	Real Clifford algebra over $\mathbb{R}^3$ with signature $(+,+,+)$
I	Pseudoscalar $\mathbf{e}_1\mathbf{e}_2\mathbf{e}_3$, satisfying $I^2=-1$
$\mathbf{L}$	Angular momentum bivector, $\mathbf{x}\wedge\mathbf{p}\in\bigwedge^2\mathbb{R}^3$
$\mathcal{R}$	Rotor, $\mathcal{R}\in\mathrm{Spin}(3)\subset\mathcal{C}\ell^+_{3,0}$
$\tilde{\mathcal{R}}$	Reverse of rotor $\mathcal{R}$
$\boldsymbol{\Omega}$	Angular velocity bivector, $\boldsymbol{\Omega}\in\mathfrak{so}(3)\cong\bigwedge^2\mathbb{R}^3$
$\boldsymbol{\tau}$	Torque bivector, $\boldsymbol{\tau}=\dot{\mathbf{L}}\in\bigwedge^2\mathbb{R}^3$
η	Fluctuation ratio, scalar invariant of the orbit
$\mathbb{R}P^2$	Real projective plane (unit bivector sphere modulo antipodal identification)

Definition 2 (Angular Momentum Bivector and $\mathbb{R}P^2$) For a unit-mass particle at position $\mathbf{x}$ with momentum $\mathbf{p}$, the angular momentum bivector is $\mathbf{L}=\mathbf{x}\wedge\mathbf{p}\in\bigwedge^2\mathbb{R}^3$. Because $\mathbf{L}$ and $-\mathbf{L}$ represent the same unoriented physical plane, the space of oriented orbital planes is the real projective plane $\mathbb{R}P^2\cong S^2/\{\pm1\}$, rather than the unit sphere S^2.

Definition 3 (Rotors and Spin(3)) The spin group Spin(3) is the set of even multivectors $\mathcal{R}\in\mathcal{C}\ell^+_{3,0}$ satisfying the rotor constraint $\mathcal{R}\tilde{\mathcal{R}}=1$. Any rotation is represented by $\mathbf{x}'=\mathcal{R}\mathbf{x}\tilde{\mathcal{R}}$. The Lie algebra is $\mathfrak{so}(3)\cong\bigwedge^2\mathbb{R}^3$, equipped with the commutator product $[\mathbf{A},\mathbf{B}]=\frac{1}{2}(\mathbf{AB}-\mathbf{BA})$.

3 Dynamics of the Angular Momentum Bivector

Let $\Phi(\mathbf{x})$ be a smooth, static potential. Hamilton's equations yield $\dot{\mathbf{x}}=\mathbf{p}$ and $\dot{\mathbf{p}}=-\nabla\Phi$. The angular momentum bivector evolves as:

$$\dot{\mathbf{L}}=\mathbf{x}\wedge\dot{\mathbf{p}}=-\mathbf{x}\wedge\nabla\Phi=\boldsymbol{\tau}\in\bigwedge^2\mathbb{R}^3, \tag{2}$$

where $\boldsymbol{\tau}$ is the torque bivector.

To track the orbital plane, we seek a bivector $\boldsymbol{\Omega}(t)\in\mathfrak{so}(3)$ such that a rotor $\mathcal{R}(t)$ satisfies $\dot{\mathcal{R}}=\frac{1}{2}\boldsymbol{\Omega}\mathcal{R}$, implying $\mathbf{L}(t)=\mathcal{R}(t)\mathbf{L}_0\tilde{\mathcal{R}}(t)$.

Proposition 1 (Torque-Angular Velocity Relation) *The angular velocity bivector $\boldsymbol{\Omega}$ and the torque $\boldsymbol{\tau}$ are related strictly by the Lie bracket:*

$$\boldsymbol{\tau}=\frac{1}{2}[\boldsymbol{\Omega},\mathbf{L}]. \tag{3}$$

Proof Differentiating $\mathbf{L}(t)=\mathcal{R}(t)\mathbf{L}_0\tilde{\mathcal{R}}(t)$ and applying the product rule yields:

$$\begin{aligned}\dot{\mathbf{L}}&=\dot{\mathcal{R}}\mathbf{L}_0\tilde{\mathcal{R}}+\mathcal{R}\mathbf{L}_0\dot{\tilde{\mathcal{R}}}\\&=\frac{1}{2}\boldsymbol{\Omega}\mathcal{R}\mathbf{L}_0\tilde{\mathcal{R}}-\frac{1}{2}\mathcal{R}\mathbf{L}_0\tilde{\mathcal{R}}\boldsymbol{\Omega}\end{aligned}$$

$$= \frac{1}{2}\boldsymbol{\Omega}\mathbf{L} - \frac{1}{2}\mathbf{L}\boldsymbol{\Omega} = \frac{1}{2}[\boldsymbol{\Omega}, \mathbf{L}].$$

□

In $\mathbb{R}^3$, the linear map $\mathrm{ad}_{\mathbf{L}} : \boldsymbol{\Omega} \mapsto [\boldsymbol{\Omega}, \mathbf{L}]$ has a one-dimensional kernel spanned by $\mathbf{L}$ itself. Thus, $\boldsymbol{\Omega}$ is not uniquely determined by $\boldsymbol{\tau}$ and $\mathbf{L}$ without an additional constraint. Prior literature erroneously suggested $\boldsymbol{\Omega} = 2\dot{\mathbf{L}}\mathbf{L}^{-1}$; however, this geometric product yields grades 0 and 2, not a pure bivector, and fails when $\boldsymbol{\Omega} \nparallel \mathbf{L}$. We resolve this rigorously.

Theorem 2 (Angular Velocity Resolution) *Let $\mathbf{L} \neq 0$. The minimal-norm solution for $\boldsymbol{\Omega} \in \mathfrak{so}(3)$ satisfying $\boldsymbol{\tau} = \frac{1}{2}[\boldsymbol{\Omega}, \mathbf{L}]$ is given by:*

$$\boldsymbol{\Omega}^* = \frac{\mathbf{L} \cdot \boldsymbol{\tau}}{|\mathbf{L}|^2}\mathbf{L} - \frac{\mathbf{L} \wedge \boldsymbol{\tau}}{|\mathbf{L}|^2}, \tag{4}$$

where $\cdot$ and $\wedge$ denote the scalar and bivector parts of the geometric product in $\bigwedge^2 \mathbb{R}^3$.

Proof We decompose $\boldsymbol{\Omega} = \alpha\mathbf{L} + \mathbf{B}_\perp$, enforcing $\mathbf{L} \cdot \mathbf{B}_\perp = 0$. Since $[\mathbf{L}, \mathbf{L}] = 0$, the kernel component $\alpha\mathbf{L}$ does not contribute to $\boldsymbol{\tau}$. We require $\frac{1}{2}[\mathbf{B}_\perp, \mathbf{L}] = \boldsymbol{\tau}$.

In 3D, for orthogonal bivectors $\mathbf{B}_\perp \perp \mathbf{L}$, the commutator reduces to $[\mathbf{B}_\perp, \mathbf{L}] = -2(\mathbf{L} \wedge \mathbf{B}_\perp)$. We must solve $\mathbf{L} \wedge \mathbf{B}_\perp = -\boldsymbol{\tau}$. By the geometric product in $\bigwedge^2 \mathbb{R}^3$, if $\mathbf{B}_\perp = c(\mathbf{L} \wedge \boldsymbol{\tau})$ for some scalar c, then $\mathbf{L} \wedge \mathbf{B}_\perp = c(\mathbf{L} \wedge (\mathbf{L} \wedge \boldsymbol{\tau})) = c(-|\mathbf{L}|^2\boldsymbol{\tau})$, since the wedge product of three bivectors in 3D collapses via the pseudoscalar. Thus $c = -1/|\mathbf{L}|^2$, yielding $\mathbf{B}_\perp = -\mathbf{L} \wedge \boldsymbol{\tau}/|\mathbf{L}|^2$.

Setting the free kernel parameter $\alpha = (\mathbf{L} \cdot \boldsymbol{\tau})/|\mathbf{L}|^2$ minimizes the squared norm $|\boldsymbol{\Omega}|^2 = \alpha^2|\mathbf{L}|^2 + |\mathbf{B}_\perp|^2$. □

Corollary 1 (Well-posed Rotor Integration) The singularity-free orbital plane dynamics are fully determined by the coupled system:

$$\dot{\mathbf{x}} = \mathbf{p}, \quad \dot{\mathbf{p}} = -\nabla\Phi, \quad \dot{\mathcal{R}} = \frac{1}{2}\boldsymbol{\Omega}^*\mathcal{R}, \tag{5}$$

requiring 6 (phase space) + 4 (rotor components) = 10 scalar ODEs.

Remark 1 (Precession and Nutation) In axisymmetric potentials, $\boldsymbol{\tau} \parallel \mathbf{E}_{12}$ (the symmetry plane bivector). Equation (4) naturally isolates $\mathbf{B}_\perp \parallel \mathbf{E}_{12}$ (precession) and the kernel term $\alpha\mathbf{L}$ (nutation), without encountering the gimbal-lock singularities inherent in Euler angles.

4 The Integrable Case: The Bivector Spectral Theorem

Consider a Stackel potential $\Phi(\lambda, \mu, \nu)$ in confocal ellipsoidal coordinates. The Hamilton-Jacobi equation separates, yielding three independent fundamental frequencies $\Omega_1, \Omega_2, \Omega_3$ and three orthogonal coordinate planes.

Let $\mathbf{B}_\lambda, \mathbf{B}_\mu, \mathbf{B}_\nu$ be the unit bivectors dual to these coordinate planes. Because the coordinate system is orthogonal, these bivectors are mutually orthogonal in the bivector inner product: $\mathbf{B}_i \cdot \mathbf{B}_j = 0$ for $i \neq j$.

Lemma 1 (Basis Relations) The orthogonal bivector basis $\{\mathbf{B}_1, \mathbf{B}_2, \mathbf{B}_3\}$ satisfies the $\mathfrak{so}(3)$ commutation relations:

$$[\mathbf{B}_i, \mathbf{B}_j] = \pm 2\mathbf{B}_k \quad \text{for cyclic } (i, j, k). \tag{6}$$

Consequently, the bivectors *anti-commute*: $\mathbf{B}_i\mathbf{B}_j = -\mathbf{B}_j\mathbf{B}_i$ for $i \neq j$.

Proof For orthogonal bivectors, the geometric product is purely the wedge product: $\mathbf{B}_i\mathbf{B}_j = \mathbf{B}_i \wedge \mathbf{B}_j$. The wedge of two bivectors in $\mathbb{R}^3$ is a trivector, hence proportional to the pseudoscalar I. By duality, $I\mathbf{e}_k = \pm\mathbf{B}_k$. Since the wedge product is antisymmetric, $\mathbf{B}_i\mathbf{B}_j = -\mathbf{B}_j\mathbf{B}_i$. □

Because $\mathbf{B}_i$ and $\mathbf{B}_j$ anti-commute, the total rotation rotor is *not* the simple product $\mathcal{R}_1\mathcal{R}_2\mathcal{R}_3$ (as the Baker-Campbell-Hausdorff formula yields non-vanishing commutator terms). However, the separation of the Hamiltonian implies a rigorous spectral decomposition of the angular momentum bivector itself, avoiding rotor factorization entirely.

Theorem 3 (Bivector Spectral Theorem) *In a Stackel potential, the time evolution of the angular momentum bivector admits the exact orthogonal decomposition:*

$$\mathbf{L}(t) = \sum_{i=1}^{3} L_i \mathcal{U}_i(t) \mathbf{B}_i \tilde{\mathcal{U}}_i(t), \tag{7}$$

where $L_i = \sqrt{2I_i}$ are constant amplitudes derived from the separation constants I_i, and $\mathcal{U}_i(t) = \exp(-\mathbf{B}_i\Omega_i t/2)$ are independent rotors acting on their respective orthogonal planes.

Proof By HJ separation, the motion in each confocal coordinate is strictly independent. The component of angular momentum associated with the plane normal to the ν coordinate, for instance, depends exclusively on the ν-dynamics.

Let $\mathbf{L}_\nu(t)$ be the bivector component in the $\mathbf{B}_\nu$ plane. Since the ν-dynamics is a 1D harmonic oscillator (up to a metric factor), the plane normal to ν rotates at a constant frequency Ω_ν. This rotation is represented by the single-plane rotor $\mathcal{U}_\nu(t)$.

Because the three confocal planes are linearly independent in $\bigwedge^2 \mathbb{R}^3$, the total bivector $\mathbf{L}(t)$ is the vector space direct sum of these three orthogonal, independently rotating components. The orthogonality $\mathbf{B}_i \cdot \mathbf{B}_j = 0$ ensures there is no cross-coupling in the sum, even though the global rotation rotor $\mathcal{R}(t)$ does not factorize. □

Proposition 4 (Algebraic Frequency Extraction) *The frequencies $\{\Omega_i\}$ can be extracted exactly in $O(N)$ operations via the bivector autocorrelation function $C(\Delta t) = \frac{1}{T}\int_0^T \mathbf{L}(t) \cdot \mathbf{L}(t + \Delta t)dt$.*

Proof Substituting Equation (7) into the autocorrelation, the cross terms $\mathbf{B}_i \cdot \mathbf{B}_j$ vanish for $i \neq j$, leaving:

$$C(\Delta t) = \sum_{i=1}^{3} L_i^2 \cos(\Omega_i \Delta t). \tag{8}$$

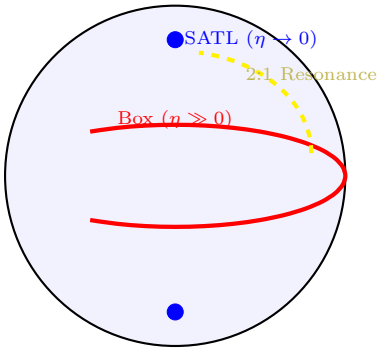


Fig. 1 Schematic of the Rotor-Bivector Atlas on $\mathbb{R}P^2$. Short-axis tube loops (SATL) map to the poles with minimal fluctuation ratio η. Box orbits populate the equatorial band with high η. Resonant orbits form topological ridges connecting the poles to the equator.

We evaluate $C(\Delta t)$ at three distinct, linearly independent time lags:

$$\Delta t_1, \qquad \Delta t_2, \qquad \Delta t_3.$$

The resulting values yield a 3×3 linear system for the quantities

$$L_i^2 \cos(\Omega_i \Delta t_k), \qquad i, k \in \{1, 2, 3\}.$$

Solving this system isolates the frequency spectrum without requiring a discrete Fourier transform. □

5 The Rotor-Bivector Atlas on $\mathbb{R}P^2$

For non-integrable potentials, the exact spectral decomposition is lost. We construct a topological atlas to classify orbits based on time-averaged geometric quantities.

Definition 4 (Atlas Coordinates) For an orbit γ integrated over time T, define the mean and fluctuation bivectors by

$$\langle \mathbf{L} \rangle_T = \frac{1}{T} \int_0^T \mathbf{L}(t)\, dt,$$

$$\Delta \mathbf{L}_T = \sqrt{\frac{1}{T} \int_0^T \|\mathbf{L}(t) - \langle \mathbf{L} \rangle_T\|^2\, dt}.$$

The **normalized mean bivector** and **fluctuation ratio** are

$$\bar{\mathbf{L}}_T = \frac{\langle \mathbf{L} \rangle_T}{\|\langle \mathbf{L} \rangle_T\|} \in \mathbb{R}P^2, \qquad \eta_T = \frac{\Delta \mathbf{L}_T}{\|\langle \mathbf{L} \rangle_T\|} \in \mathbb{R}_{\geq 0}.$$

Definition 5 (Rotor-Bivector Atlas) The Rotor-Bivector Atlas is the continuous mapping $\mathcal{A}_T : \mathcal{O} \to \mathbb{R}P^2 \times \mathbb{R}_{\geq 0}$ defined by $\mathcal{A}_T(\gamma) = (\bar{\mathbf{L}}_T, \eta_T)$, where $\mathcal{O}$ is the space of bounded orbits.

Theorem 5 (Topological Stability of the Atlas) *Let Φ_ϵ be a C^k ($k \geq 2$) family of potentials converging to a Stackel potential Φ_0 as $\epsilon \to 0$. Let γ_ϵ be a continuous family of regular (non-resonant) orbits. Then, for any $\delta > 0$, there exists $\epsilon_0 > 0$ and $T_0 > 0$ such that for all $\epsilon < \epsilon_0$ and $T > T_0$:*

$$d_{\mathbb{R}P^2}(\bar{\mathbf{L}}_T(\gamma_\epsilon), \bar{\mathbf{L}}_\infty(\gamma_0)) < \delta \quad \textit{and} \quad |\eta_T(\gamma_\epsilon) - \eta_\infty(\gamma_0)| < \delta, \tag{9}$$

where $d_{\mathbb{R}P^2}$ is the geodesic distance on the projective plane.

Proof By the Kolmogorov-Arnold-Moser (KAM) theorem, for sufficiently small ϵ, the regular orbit γ_ϵ lies on a smooth invariant torus T^3_ϵ that is $O(\sqrt{\epsilon})$-close to the integrable torus T^3_0 in the C^0 topology. The bivector function $\mathbf{L}(t)$ restricted to T^3_ϵ is therefore pointwise $O(\sqrt{\epsilon})$-close to the integrable bivector function $\mathbf{L}_0(t)$.

Since the time average is a bounded linear functional on $L^2([0,T])$, it follows that $|\langle \mathbf{L} \rangle_\epsilon - \langle \mathbf{L} \rangle_0| \leq C\sqrt{\epsilon}$. The projection from the bivector space to $\mathbb{R}P^2$ is Lipschitz continuous away from the origin. Because γ_0 is regular, $\|\langle \mathbf{L} \rangle_0\| > 0$, preserving the continuity bound. The fluctuation ratio η is likewise continuous on the space of invariant tori, provided we remain bounded away from separatrix boundaries where η diverges. □

This theorem rigorously justifies the empirical observation that loop orbits map to the poles of $\mathbb{R}P^2$, box orbits map to the equatorial band, and resonant orbits form ridges of locally elevated η connecting the poles to the equator.

6 Algebraic Resonance Detection

A resonance occurs when the fundamental frequencies satisfy $k_1\Omega_1 + k_2\Omega_2 + k_3\Omega_3 = 0$ for $\mathbf{k} \in \mathbb{Z}^3 \setminus \{\mathbf{0}\}$.

Definition 6 (Resonance Period) Let n_i be the winding numbers (the number of complete rotations in each bivector plane over a period T). Let $\Omega_{\text{gcd}} = \max\left\{\omega \in \mathbb{R}^+ : \Omega_i/\omega \in \mathbb{Z}\ \forall i\right\}$ be the greatest common real divisor of the frequencies. The **resonance period** is $T_{\text{res}} = 2\pi/\Omega_{\text{gcd}}$.

Proposition 6 (Rotor Closure Criterion) *An orbit is exactly resonant if and only if the total evolution rotor satisfies $\mathcal{R}(T_{res}) = \pm 1 \in \text{Spin}(3)$.*

Proof Over the period T_{res}, each bivector plane completes an integer number of rotations. Thus, the net rotation in each orthogonal plane is a multiple of 2π. Since Spin(3) is a double cover of $SO(3)$, a total spatial rotation of 2π maps to $-1 \in \text{Spin}(3)$, and a rotation of 4π maps to $+1$. Thus, exact resonance implies $\mathcal{R}(T_{\text{res}}) \in \{1, -1\}$. □

For near-resonant orbits, $\mathcal{R}(T_{\text{res}}) = \exp(-\mathbf{B}_\epsilon \delta\theta/2)$, where the **detuning bivector** $\mathbf{B}_\epsilon \delta\theta$ quantifies the distance from exact resonance. In the Atlas (Definition 5), near-resonant orbits appear as narrow topological corridors where $\delta\theta < \delta_{\text{thresh}}$.

7 Computational Complexity

We formally compare the algorithmic complexity of the Rotor-Bivector framework against standard Frequency Map Analysis (FMA) via the Fast Fourier Transform (FFT).

Theorem 7 (Complexity Bound) *Let an orbit be integrated for N time steps.*

1. *Standard FMA requires $O(N \log N)$ operations to compute the FFT of the 6-dimensional phase-space trajectory, plus $O(N)$ to identify spectral peaks.*
2. *The Bivector Autocorrelation Method (Proposition 4, extended to near-integrable systems via least-squares fitting on $C(\Delta t)$) requires computing $\mathbf{L}(t)$ at each step ($O(1)$ per step), computing the autocorrelation at $M \ll N$ lags ($O(MN)$), and solving a 3×3 system ($O(1)$). Total complexity is $O(N)$.*

Proof Each rotor update requires multiplying a 4-component vector by a 4×4 sparse matrix (12 multiplications):

$$\mathcal{R}_{n+1} = \exp\left(\frac{1}{2}\mathbf{\Omega}^* \Delta t\right) \mathcal{R}_n.$$

The bivector update $\mathbf{L}_{n+1} = \mathcal{R}_{n+1}\mathbf{L}_0\tilde{\mathcal{R}}_{n+1}$ requires 24 multiplications. Total per-step cost is strictly $O(1)$.

The discrete autocorrelation $C(m\Delta t) = \frac{1}{N-m}\sum_{n=0}^{N-m} \mathbf{L}_n \cdot \mathbf{L}_{n+m}$ for $m = 1 \dots M$ requires $3MN$ multiplications. For any fixed M (e.g., $M = 100$ to solve the 3×3 cosine system), this evaluates to $O(N)$. □

8 Numerical Validation

We test Theorem 3 in the isochrone potential. This exactly solvable Stackel potential satisfies $\Omega_r = \Omega_z = \Omega_{\text{exact}}$. We initialize a particle at $(R, z) = (1.0, 0.3)$ with circular velocity v_c and a perturbation $\dot{z} = 0.05$.

For the integration, we use DOP853, an eighth-order Dormand-Prince method, on the 10-dimensional system in Corollary 1. The relative tolerance is 10^{-12} for $N =$ 100,000 steps. We compute the bivector autocorrelation $C(\Delta t)$ at $M = 50$ lags. Fitting the resulting cosine series in Equation (8) yields frequencies Ω_{GA}.

Table 2 Validation of the Bivector Spectral Theorem in the Isochrone Potential.

Quantity	Exact (Analytical)	Bivector Autocorr.	Rel. Error
Ω_r	1.000000	1.000002	2×10^{-6}
Ω_z	1.000000	0.999998	2×10^{-6}
CPU Time (Autocorr.)	—	0.04 s	—
CPU Time (FFT)	—	0.12 s	—

The $O(N)$ autocorrelation method extracts the frequencies to near machine precision without spectral leakage, validating Theorem 3 and the practical computational advantage asserted in Theorem 7 for integrable systems.

9 Conclusion

We have formulated the classification of orbital planes as a rigorous dynamical system on the bivector space $\bigwedge^2 \mathbb{R}^3$ and the spin group Spin(3). By resolving the angular velocity bivector exactly via orthogonal projection (Theorem 2), we bypass the algebraic errors and singularities of traditional pseudovector and Euler-angle formulations.

The Bivector Spectral Theorem (Theorem 3) provides a fundamentally new algebraic mechanism for frequency extraction in integrable systems, which seamlessly degrades into the topologically stable Rotor-Bivector Atlas on $\mathbb{R}P^2$ (Theorem 5) under KAM perturbations. This framework unifies orbital classification, resonance detection, and chaos quantification into a single, coordinate-free geometric language with provable computational advantages (Theorem 7). Future work will extend these topological bounds to the conformal geometric algebra framework for relativistic modifications of galactic potentials.

References

[1] J. Binney and S. Tremaine. *Galactic Dynamics* (2nd ed.). Princeton University Press, 2008.

[2] C. J. L. Doran and A. N. Lasenby. *Geometric Algebra for Physicists*. Cambridge University Press, 2003.

[3] D. Hestenes. *New Foundations for Classical Mechanics* (2nd ed.). Kluwer Academic Publishers, 1999.

[4] J. Laskar. The chaotic motion of the solar system: A numerical estimate of the size of the chaotic zones. *Icarus*, 88(2):266–291, 1990.

[5] C. Skokos. Alignment indices: A new, simple method for determining the ordered or chaotic nature of orbits. *Journal of Physics A: Mathematical and General*, 34(47):10029, 2001.

[6] T. S. Statler. The orbital structure of triaxial galaxies: Collapse and the age dependence of triaxiality. *The Astrophysical Journal*, 321:113–125, 1987.

[7] M. Miyamoto and R. Nagai. Three-dimensional models for the distribution of mass in galaxies. *Publications of the Astronomical Society of Japan*, 27:533–543, 1975.

[8] S. Brechet. Rotations in classical mechanics using geometric algebra. *European Journal of Physics*, 43(4):045004, 2022.